Supporting Information

Third-Order Optical Nonlinearities of Two-dimensional SnS under Irradiation: Implications for Space Use

Shu-Yan Wang, Xiao-Juan Zhen, Zhan-Zu Feng, Ming-Jun Xiao, Shi-Ji Li, Wen Shang, Yi-Fan Huang, [*] Qiang Wang, [*] and Hao-Li Zhang [*]

Corresponding Authors:

Qiang Wang, E-mail: qiangwang@lzu.edu.cn

Hao-Li Zhang, E-mail: haoli.zhang@lzu.edu.cn

Yi-Fan Huang, E-mail: yifanhuang@lzcu.edu.cn

Spectroscopic measurements

UV/Vis/NIR absorption spectra were collected on a TU-1810 spectrophotometer (Beijing Purkinje General Instrument, China) and the diffuse reflectance spectra were recorded on a Shimadzu UV Probe 2600 equipped with an integrating sphere ($BaSO_4$ as the reference). Fourier transform infrared spectroscopy (FTIR) was performed on a VERTEX 70/80 V FTIR spectrometer (Bruker, Germany) using the KBr pellet technique. For femtosecond broadband pump-probe spectroscopy, the laser source was a Coherent Legend Elite regenerative amplifier (1 kHz, 800 nm), which was seeded by a Coherent Chameleon oscillator (120 fs, 80 MHz). 800 nm wavelength laser pulses were from the regenerative amplifier's output while 400 nm pulses were obtained by doubling the fundamental 800 nm pulses with a BBO crystal. Other pump wavelengths were generated from a Light Conversion OPerA-Solo optical parametric amplifier (290-2600 nm). The available broadband probe wavelength was from the UV to the NIR range (350-1600 nm).
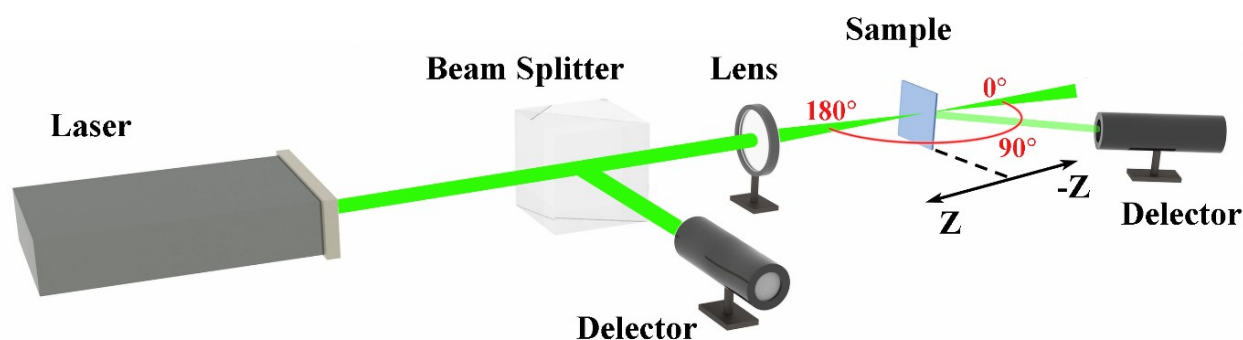
Z-scan measurements
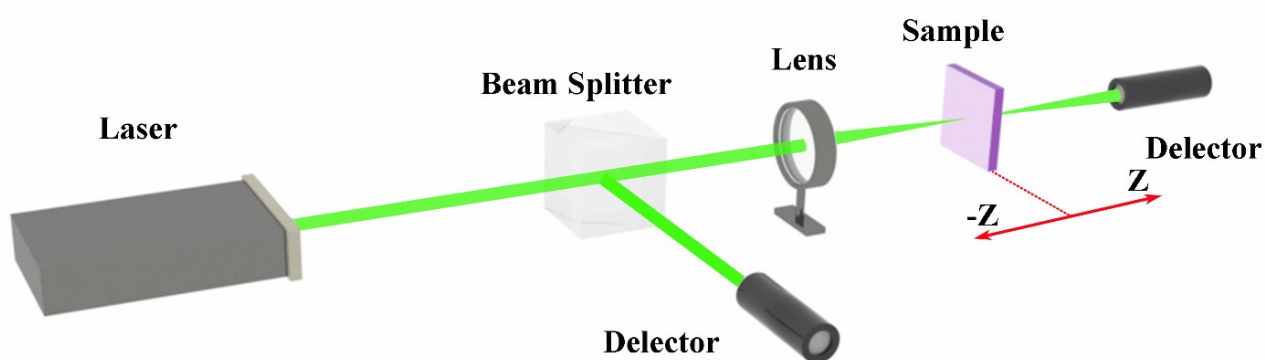
Scheme S1. Z-scan Setup

Nanosecond Z-scan measurements were performed on a Q-switched Nd: YAG laser (Continuum Surelite SL-I-10) with two output wavelengths of 532 and 1064 nm (~4 ns, 10 Hz). Under the open-aperture conditions, the normalized transmittance is measured as the

sample translates through the focal plane of the focused beam. A normalized transmittance above 1 indicates that the sample exhibits saturable absorption.

The fs Z-scan setup employs the above-mentioned fs laser as the light source.

Nonlinear scattering measurement: With the same Z-scan setup, but the detector is placed at an angle offset from the incident beam to collect the scattering signal.

Scheme S2. Nonlinear scattering measurement setup

I-scan measurement: With the same Z-scan setup, but the sample is fixed at the focus position of the optical path of the apparatus. The normalized transmittance of the sample as a funtion of the input fluence (energy) is measured by using a 532 nm laser output.

Other characterizations

The X-ray powder diffraction (XRD) patterns of SnS nanoflowers were recorded on a PANalytical X'Pert PRO powder diffractometer from ~10 to 90° 2θ using Cu K_{α} radiation (graphite monochromator, λ=1.5418 Å) at room temperature. The morphology of samples was collected on field-emission scanning electron microscopy (SEM, Apreo S). The TEM micrographs were obtained using Tecnai G2 F30 and Talos F200C Field Emission Transmission Electron Microscopes (FEI, USA) at operating voltage of 300 and 200 kV, respectively. The samples were dispersed onto holey carbon grids with the evaporation of the excess solvent. X-ray photoelectron spectroscopic (XPS) measurements were performed on an

AXIS Ultra instrument. The Raman spectroscopy data is collected using the Renishaw inVia Raman microscope at the excitation wavelength of 785 nm.
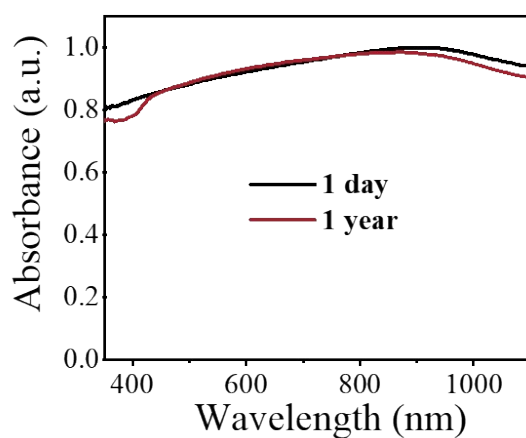

Figure S1. Absorbance evolution of the SnS over a long period of more than one year.
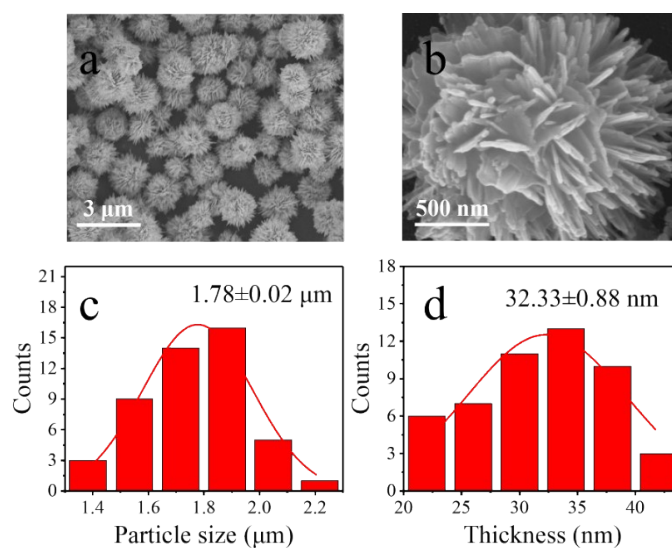

Figure S2. The SEM images of SnS (a, b). The histograms of the sphere diameter of 1.78±0.02 μm (c) and the thickness of 32.33±0.88 nm (d) based on the statistical data of 50 samples.
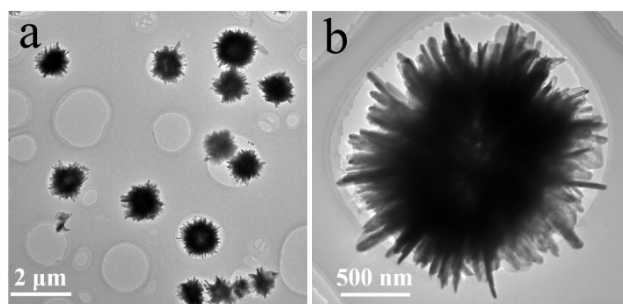
Figure S3. More TEM spectra of SnS with different resolution. The synthesized SnS has flower-like structure and uniform particle size.
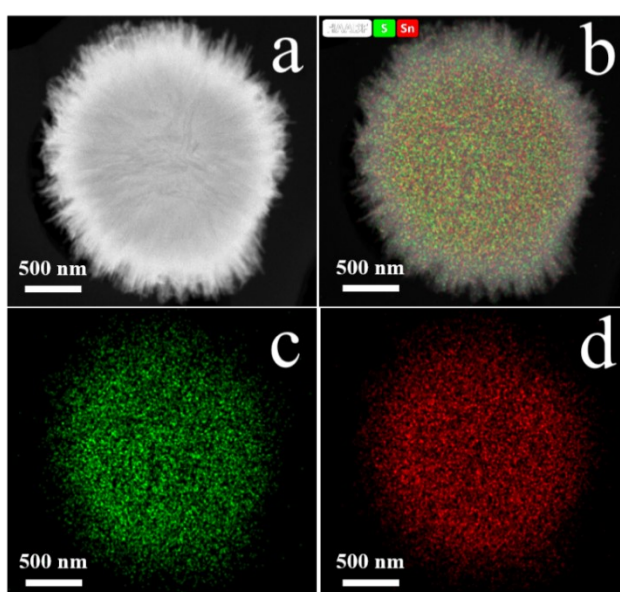

Figure S4. Element distribution mapping of SnS. a) high-angle annular dark field (HADDF) images.b) S and Sn Elements. c) S and d) Sn , respectively.
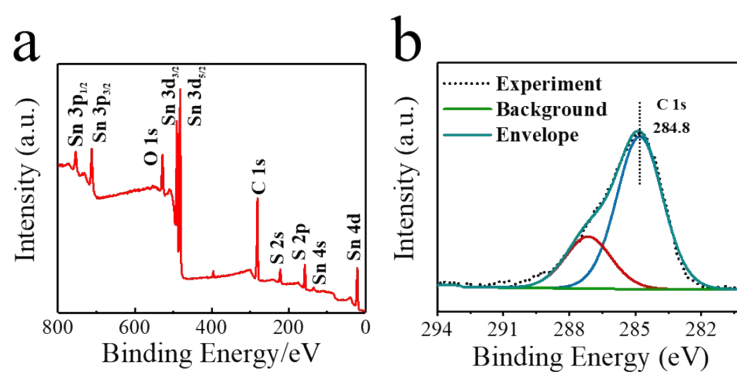

Figure S5. XPS of SnS: a) XPS survey spectra of the SnS, b) C 1s spectra used for the calibration of the data.
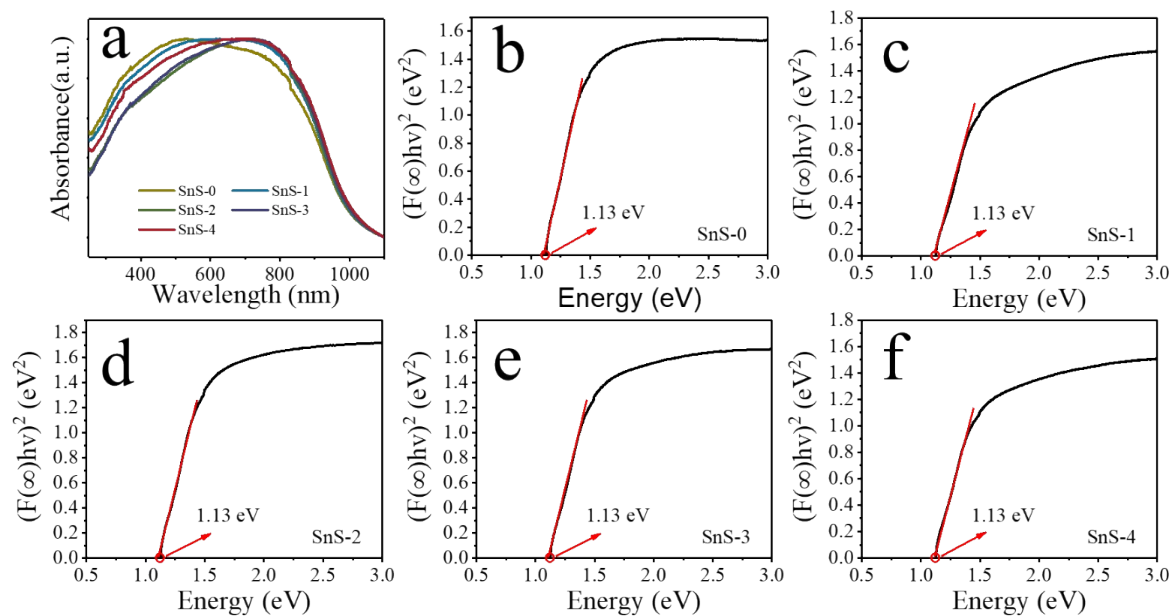
Figure S6. a) The UV-Vis-Nir diffuse reflection spectra and corresponding Tauc plots of b) SnS-0, c) SnS-1, d) SnS-2, e) SnS-3, and f) SnS-4..
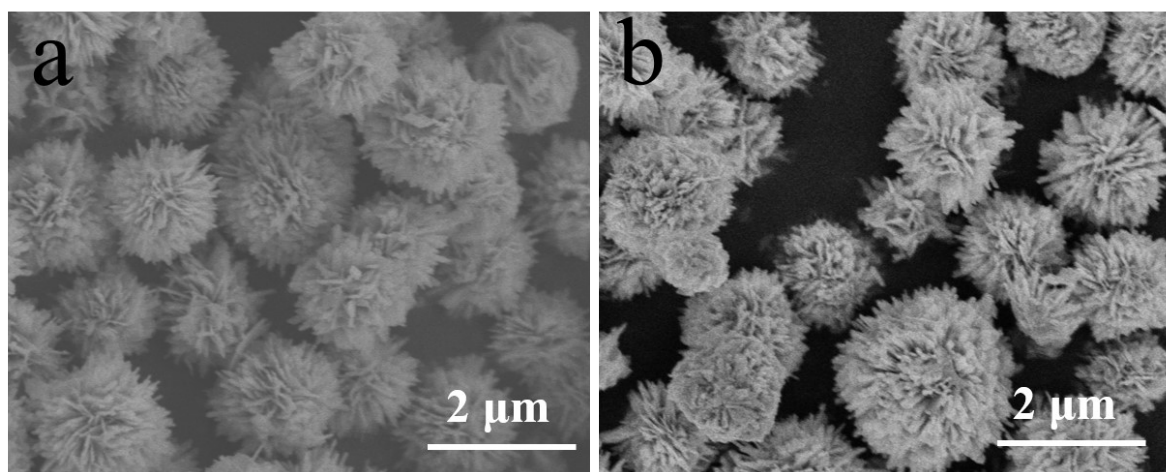

Figure S7. The SEM spectra of the SnS nanosheets a) before and b) after irradiation by ^{60}Co γ-rays.
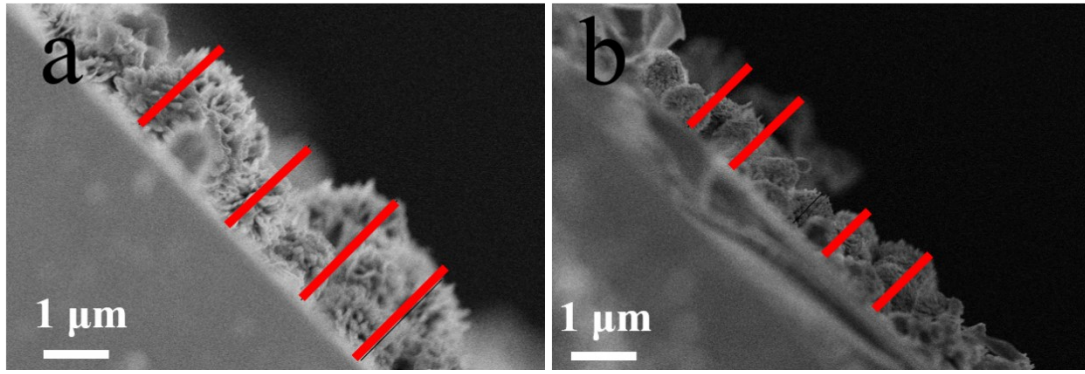
Figure S8. More SEM spectra of SnS films. The thickness of pristine SnS films is ~2 μm.
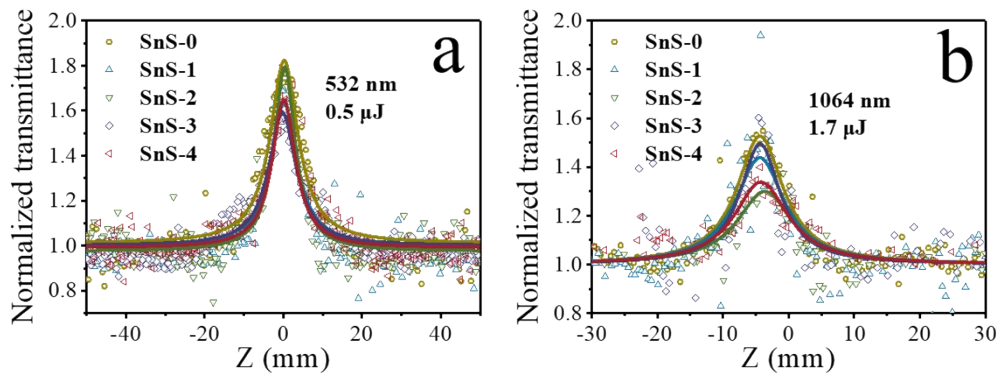

Figure S9. Open aperture ns Z-scan data for the SnS-0, SnS-1, SnS-2, SnS-3, and SnS-4 films with a similar linear transmittance of ~0.35 at the excitation of a) 532 nm, 0.5 μJ and b) 1064 nm, 1.7 μJ respectively.

Table S1. Summary of the fitted nonlinear optical parameters for the open aperture ns Z-scan for the SnS-0, SnS-1, SnS-2, SnS-3, and SnS-4 films.

Samples	ns λ_{laser} E_{laser}	T	β (m·W^{-1})	*Delta	Samples	ns λ_{laser} E_{laser}	T	β (m·W^{-1})	*Delta
SnS-0		0.31	-2.83×10^{-6}	—	SnS-0		0.34	-5.45×10^{-7}	—
SnS -1	532 nm 0.5 μJ	0.38	-2.11×10^{-6}	-25.4%	SnS -1	1064 nm 1.7 μJ	0.37	-4.97×10^{-7}	-8.8%
SnS -2		0.33	-2.35×10^{-6}	-17.0%	SnS -2		0.37	-4.37×10^{-7}	-19.8%
SnS -3		0.34	-2.16×10^{-6}	-23.7%	SnS -3		0.33	-4.51×10^{-7}	-17.2%
SnS -4		0.35	-2.09×10^{-6}	-26.1%	SnS -4		0.34	-4.42×10^{-7}	-18.9%
SnS-0		0.39	-1.94×10^{-6}	—	SnS-0		0.33	-6.89×10^{-7}	—
SnS -1	532 nm 0.8 μJ	0.36	-1.86×10^{-6}	-4.1%	SnS -1	1064 nm 2.6 μJ	0.37	-6.12×10^{-7}	-11.2%
SnS -2		0.35	-1.73×10^{-6}	-10.8%	SnS -2		0.40	-5.68×10^{-7}	-17.6%
SnS -3		0.35	-1.79×10^{-6}	-7.7%	SnS -3		0.43	-5.75×10^{-7}	-16.5%
SnS -4		0.31	-1.70×10^{-6}	-12.4%	SnS -4		0.34	-5.71×10^{-7}	-17.1%

*Delta represents the degradation percentage of the decrease of the nonlinear absorption coefficient β relative to SnS-0 of the irradiated sample.
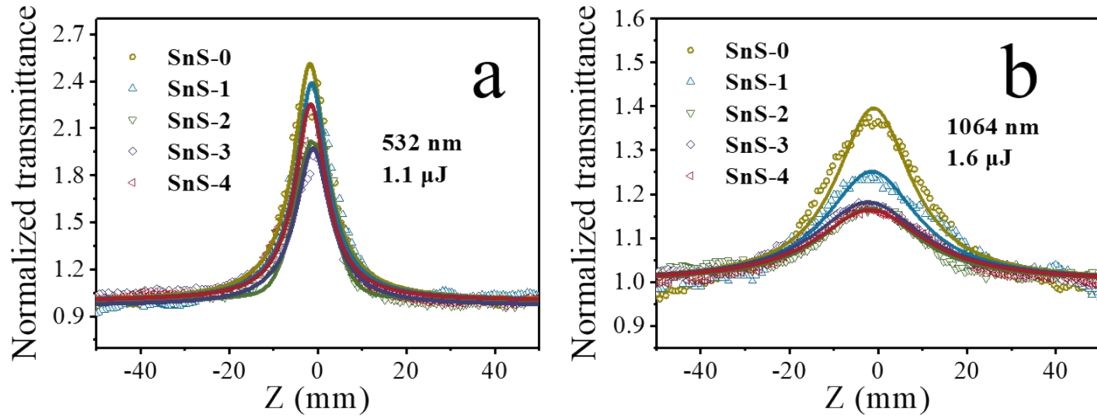
Figure S10. Open aperture fs Z-scan data for the SnS-0, SnS-1, SnS-2, SnS-3 and SnS-4 films with a similar linear transmittance of ∼0.30 at the excitation of a) 532 nm, 1.1 µJ and b) 1064 nm, 1.6 µJ respectively.

Table S2. Summary of the fitted nonlinear optical parameters for the open aperture fs Z-scan for the SnS-0, SnS-1, SnS-2, SnS-3, and SnS-4 films.

Samples	fs λ_{laser} E_{laser}	T	β (m·W⁻¹)	*Delta	Samples	fs λ_{laser} E_{laser}	T	β (m·W⁻¹)	*Delta
SnS-0		0.43	-3.59×10^{-9}	—	SnS-0		0.36	-2.05×10^{-9}	—
SnS -1	532 nm 0.4 µJ	0.41	-2.99×10^{-9}	-16.7%	SnS -1	1064 nm 1.6 µJ	0.39	-1.69×10^{-9}	-17.6%
SnS -2		0.43	-2.85×10^{-9}	-20.6%	SnS -2		0.33	-1.26×10^{-9}	-38.5%
SnS -3		0.44	-2.62×10^{-9}	-27.0%	SnS -3		0.38	-1.49×10^{-9}	-27.3%
SnS -4		0.45	-2.78×10^{-9}	-22.6%	SnS -4		0.40	-1.36×10^{-9}	-33.7%
SnS-0		0.31	-7.28×10^{-9}	—	SnS-0		0.36	-2.16×10^{-9}	—
SnS -1	532 nm 1.1 µJ	0.53	-6.45×10^{-9}	-11.4%	SnS -1	1064 nm 2.6 µJ	0.39	-1.99×10^{-9}	-7.9%
SnS -2		0.35	-5.69×10^{-9}	-21.8%	SnS -2		0.33	-1.88×10^{-9}	-13.0%
SnS -3		0.47	-5.51×10^{-9}	-24.3%	SnS -3		0.43	-1.56×10^{-9}	-27.8%
SnS -4		0.52	-5.92×10^{-9}	-18.7%	SnS -4		0.37	-1.72×10^{-9}	-20.4%

*Delta represents the degradation percentage of the decrease of the nonlinear absorption coefficient β relative to SnS-0 of the irradiated sample.
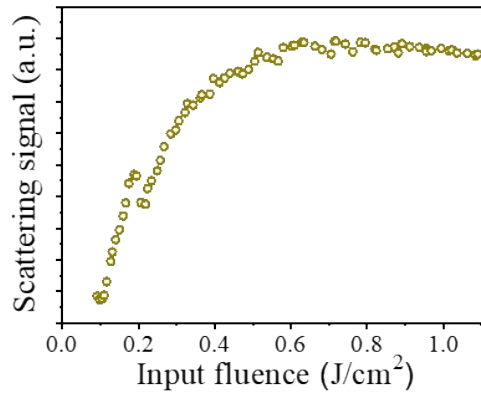

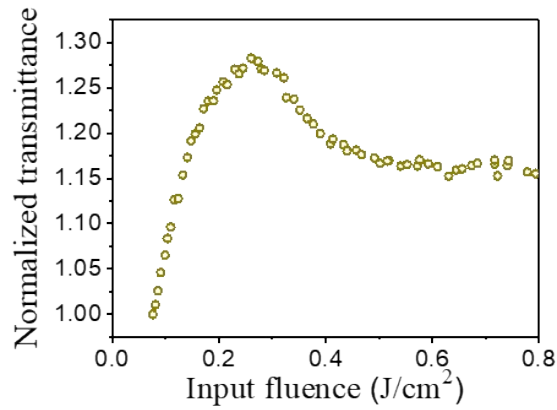**Figure S11**. At the angle of 5°, the dependence of the scattering rate on the incident fluence was measured.

Figure S12. The normalized transmittance of the sample as a funtion of the input fluence measured by using a 532 nm laser output.
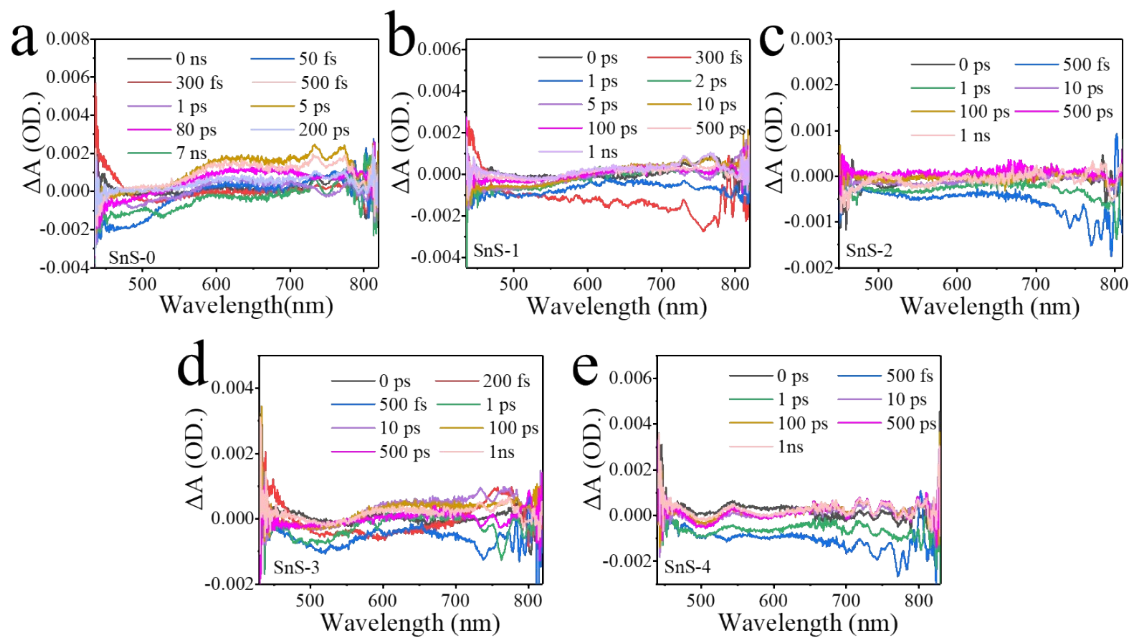

Figure S13. Representative decay curves of a) SnS-0, b) SnS-1, c) SnS-2, d) SnS-3 and e) SnS-4 (the pump excitation wavelength was 400 nm).
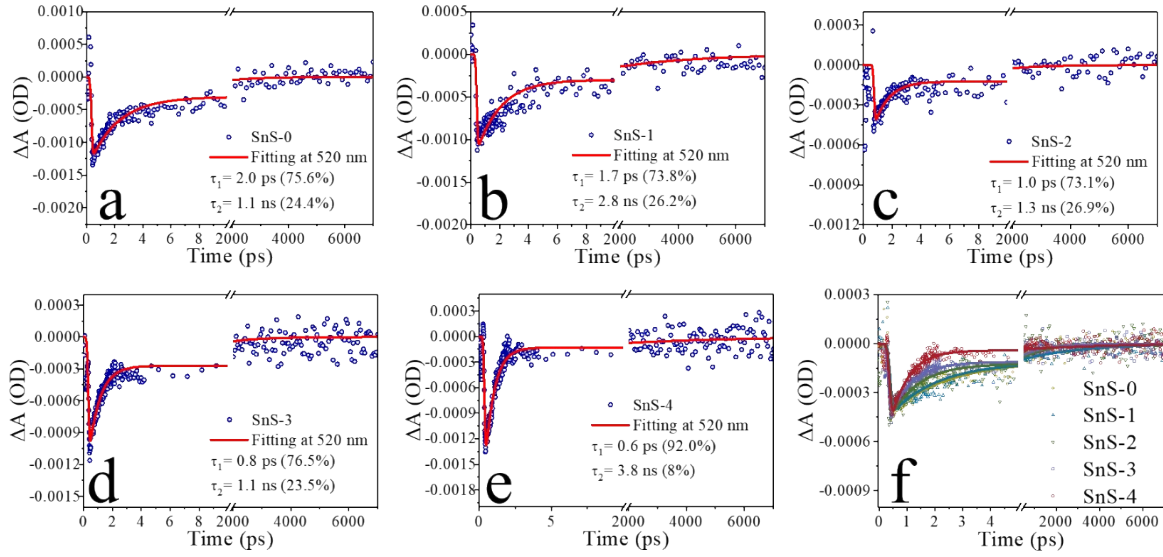
Figure S14. The kinetic traces of a) SnS-0, b) SnS-1, c) SnS-2, d) SnS-3, e) SnS-4 at 520 nm and f) the overlapping (normalized) for comparison (the pump excitation wavelength was 400 nm).

Table S3. Summary of the fitted fs transient absorption data of SnS, SnS-1, SnS-2, SnS-3 and SnS-4 films.

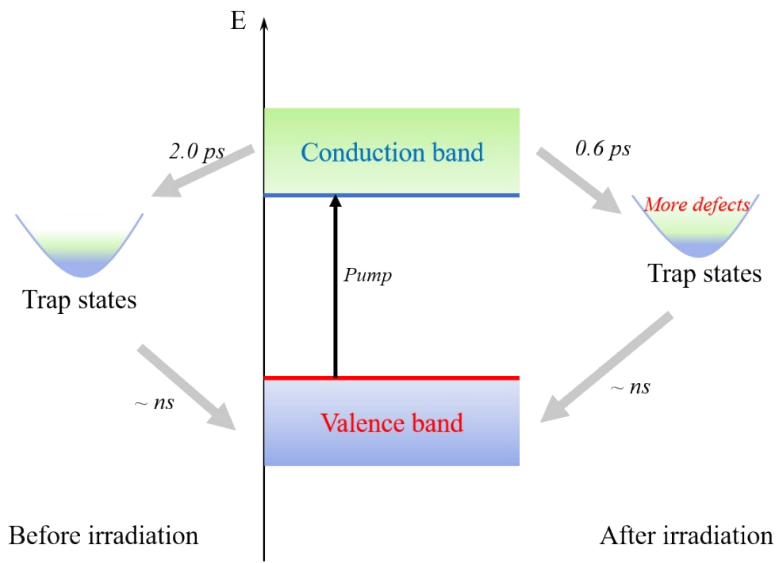| Samples	Probe wavelength	τ_1	τ_2
SnS-0	520 nm	2.0 ps (75.6%)	1.1 ns (24.4%)
SnS-1	520 nm	1.7 ps (73.8%)	2.8 ns (26.2%)
SnS-2	520 nm	1.0 ps (73.1%)	1.3 ns (26.9%)
SnS-3	520 nm	0.8 ps (76.5%)	1.1 ns (23.5%)
SnS-4	520 nm	0.6 ps (92.0%)	3.8 ns (8.0%)

Figure S15. The schematic carrier dynamics of SnS before and after irradiation.